Fast-responsive capsule based on two soluble components for self-healing concrete

Gao, Jian; Jin, Peng; Zhang, Yuze; Dong, Hua; Wang, Ruixing

DOI
10.1016/j.cemconcomp.2022.104711

Publication date
2022

Document Version
Final published version

Published in
Cement and Concrete Composites

Cement and Concrete Composites 133 (2022) 104711

Contents lists available at ScienceDirect

Cement and Concrete Composites

journal homepage: www.elsevier.com/locate/cemconcomp

Fast-responsive capsule based on two soluble components for self-healing concrete

Jian Gao [a,b], Peng Jin [a,b], Yuze Zhang [a,b], Hua Dong [c,**], Ruixing Wang [a,b,*]

[a] School of Materials Science and Engineering, Southeast University, Nanjing, 211189, China
[b] Jiangsu Key Laboratory of Construction Materials, Southeast University, Nanjing, 211189, China
[c] Microlab, Faculty of Civil Engineering and Geoscience, Delft University of Technology, Delft, the Netherlands

ARTICLE INFO

Keywords:
Fast-responsive capsule
Composite-wall structure
Self-healing
Double-component

ABSTRACT

Due to low activity or long mineralization time, traditional mineral agents for self-healing concrete generally need a long time to achieve a desired repair efficiency. Inspired by epoxy resin AB glue which can consolidate in a short time when mixing the two components together, a novel type of fast-responsive capsules based on two soluble components was designed for self-healing concrete. Component A (sodium carbonate) and component B (calcium acetate) were encapsulated in two different groups of capsules, respectively, coated with three layers consisting of epoxy resin and fine sands to achieve superior waterproof and alkali resistance properties. After rupture of the capsules, the rapid response with respect to core material dissolution and precipitation can be realized in presence of water, by which the cracks below 200 μm can be healed in 3 days. Super absorbent resin (SAP) embedded in the capsules could expand in contact with water, and further improve the self-healing efficiency of the capsules by blocking the crack.

1. Introduction

Concrete is the most important civil engineering material owing to its low cost and proper overall performance. However, concrete, as a brittle composite cementitious material, is prone to crack due to mechanical loads or exposure to aggressive environments. Furthermore, cracks promote the ingress of detrimental agents such as chloride and sulfate ions, which would accelerate the concrete deterioration and rebar corrosion, thus greatly shortening the service life of concrete [1–5].

In the past years, self-healing concrete has attracted extensive interest for sustainable constructions. Traditional concrete has been found to have a autogenous self-healing capacity due to further hydration of cement particles and carbonation of calcium hydroxide leached from the matrix [3,6,7], while the efficiency of autogenous healing is rather limited [8,9]. Therefore, some innovative materials, such as bacteria [10,11], superabsorbent polymers (SAP) [12], polymer adhesive agents [13], and mineral admixtures [14,15], have been extensively explored for self-healing concrete.

Bacteria can promote the precipitation of calcium carbonate in cracks by degrading urea to produce carbonate [7] or capturing carbon dioxide from the air [16]. Several studies showed that impermeability, strength, and maximum width of healable crack can be improved with the bacteria series [10,17,18]. Despite being encapsulated or immobilized in a protective carrier beforehand, bacterial activity and survival time are limited [19,20] due to high pH (over 12) and densification of pore structure [21]. Another problem is that nutrients for bacterial development like extract yeast [22] and sucrose [23]might cause retardation of cement hydration.

Superabsorbent polymers (SAP) can expand up to hundreds of times their original volume because of the cross-linked hydrophilic structure. Hence, SAP can be used to heal concrete cracks since it promotes rehydration with absorbed water [24] and improves impermeability of concrete [25]. However, the mechanical properties of concrete mixed with SAP could be reduced due to macro-pore formation [26].

Polymer adhesive agents, such as the combination of epoxy resin and hardener, can seal and bridge cracks. The two components (i.e., epoxy resin and hardener) are usually stored separately in different groups of microcapsules for a desired shelf life in concrete. When microcapsules break upon the formation of cracks in the cement matrix, the two components are released to the cracks and heal the cracks after hardening. Although polymer adhesive agents can repair cracks quickly, they

* Corresponding author. School of Materials Science and Engineering, Southeast University, Nanjing, 211189, China.
** Corresponding author.
E-mail address: ruixing@seu.edu.cn (R. Wang).

https://doi.org/10.1016/j.cemconcomp.2022.104711
Received 30 March 2022; Received in revised form 27 June 2022; Accepted 3 August 2022
Available online 12 August 2022

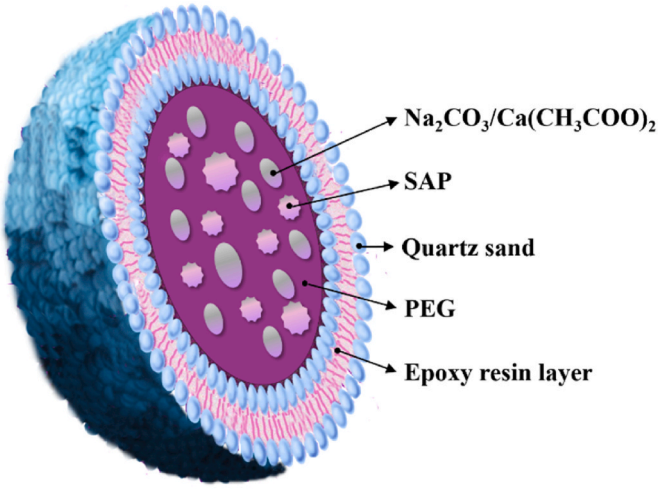

Fig. 1. Structure diagram of self-healing capsule.

are mostly expensive and incompatible with cement matrix. Moreover, a proper mixing of the two-part adhesives in the cracks is difficult to ensure, which may lead to unsatisfactory polymerization [27].

The mineral admixtures are inorganic materials, their reaction products have good compatibility with cementitious matrix, showing an advantage over bacteria and adhesives as healing agents. For example, the expansive powder minerals (magnesium oxide, bentonite, and quicklime) were encapsulated in concentric glass macrocapsules for self-healing concrete and could seal the cracks within a range of 360–380 μm after a 28-day healing time [28]. The compounds of silicon dioxide, montmorillonite clay, and sodium aluminum silicate hydroxide were also studied [29]. It has been reported that the water tightness [30] and mechanical properties [31] could be improved considerably after healing. However, these traditional mineral admixtures usually have a poor mobility in cracks and require a long time to achieve a stable repair effect. During this process, aggressive ions like Cl^- can diffuse continuously into the concrete through incompletely healed cracks, which extremely shortens the service life of concrete. Hence, it is profound to research some mineral admixtures, such as sodium carbonate and calcium acetate, that can seal the cracks quickly. In order to maintain the potential of these mineral admixtures, techniques of encapsulation have been extensively investigated already. For instance, hollow glass fibre and polymer microcapsule can protect the minerals effectively.

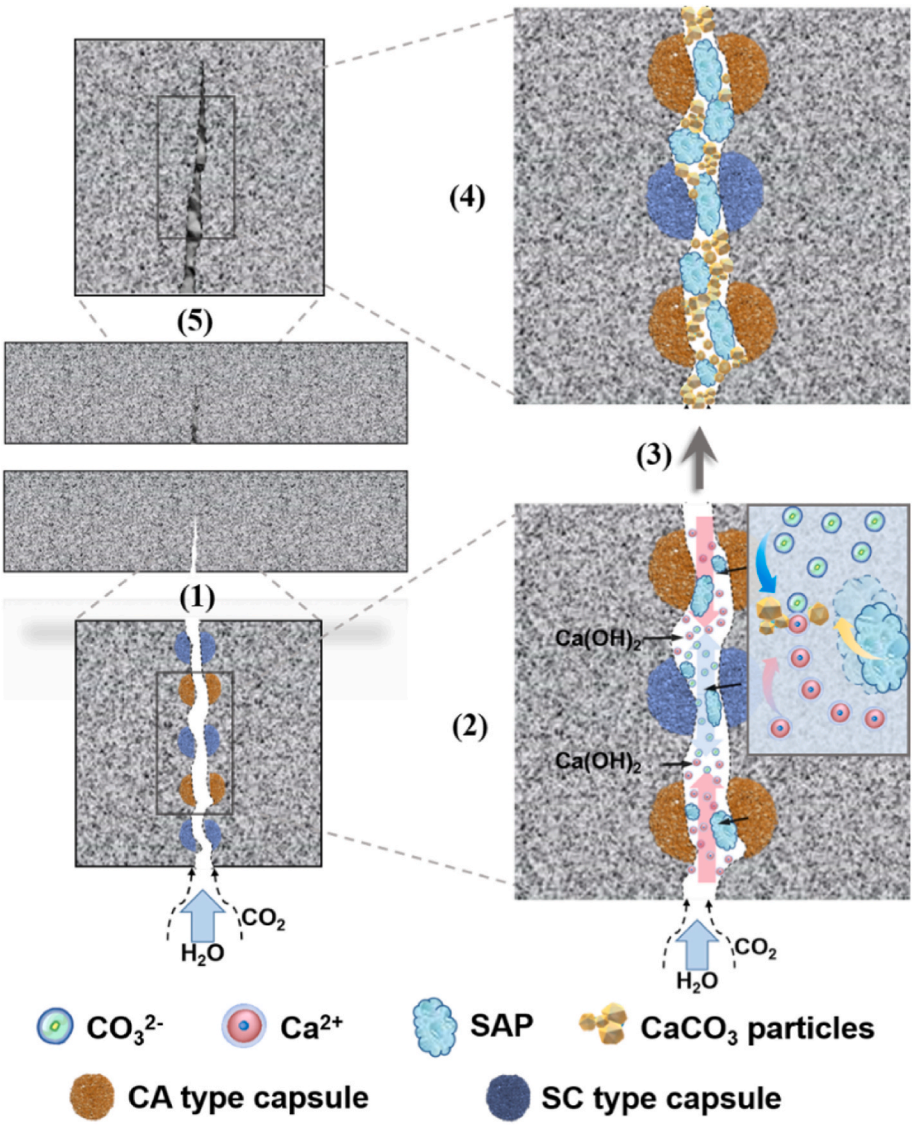

Fig. 2. Schematic illustration for the application of double-capsule healing system (Refer to Table 2 for CA/SC type capsule). (1) The cracking of concrete and the entry of water and CO_2 from outside; (2) The dissolution of core materials could release Ca^{2+}, CO_3^{2-}, and SAP, which could migrate and swell in presence of water; (3) The consequent interaction of Ca^{2+} with CO_3^{2-} leads to the formation of $CaCO_3$ particles to fill between SAP, and then both seal the crack; (4) The synergistic effect of $CaCO_3$ particles and SAP could promote the crack repair.

Table 1
Chemical composition of cement (wt%).

Oxide	CaO	SiO_2	Al_2O_3	SO_3	Fe_2O_3	MgO	K_2O	Others
Composition(%)	62.66	21.61	5.74	3.76	3.19	1.83	0.76	0.45

Table 2
Mix composition of capsules.

Type of capsule	Core materials				Wall materials	
	Sodium carbonate	Calcium acetate	PEG	SAP	Epoxy mixture	Fine sand
SC	1.00	–	1.00	0.1	0.20	0.50
CA	–	1.00	1.70	0.1	0.27	0.67
CC	1.00	0.80	2.23	0.18	0.40	1.01

Table 3
Description of different types of capsules.

Types of capsules	Structure	Purpose
CA-A SC-A CC-A	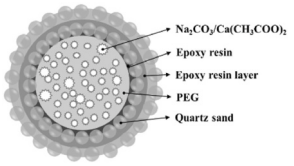	To research the effect of SAP
CA-B SC-B CC-B	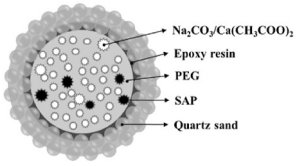	To research the difference between double-wall structure and composite-wall structure
CA-C SC-C CC-C	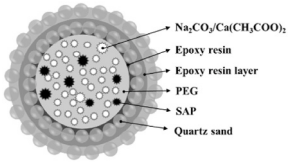	To research the difference between double-wall structure and composite-wall structure

Nonetheless, the proper dispersion of the hollow glass fibre in concrete is challenging [32], and the bond between the polymer microcapsule and the concrete matrix is usually weak [33]. By contrast, the granulation/film coating technology seems to be promising due to its simplicity and relatively large capacity to store the mineral healing agents [34,35].

In this study, a type of fast-responsive capsules based on two soluble components (i.e., sodium carbonate (Na_2CO_3), calcium acetate ($Ca(CH_3COO)_2$)) is developed for self-healing concrete. Superabsorbent polymers (SAP) is also incorporated in the capsules to enhance the cracking healing efficiency. Poly (ethylene glycol) (PEG), which is a phase change material with excellent solubility in water, is used for granulation. The PEG is in liquid form at elevated temperature and binds the crystal powders together. Then the bulk material becomes solid while cooling down. The wall material composed of epoxy resin and fine sand (Fig. 1) is designed to ensure the waterproof property of the capsules. A pure epoxy resin layer is introduced between two quartz sand layers. Thus, the core material can be well preserved in concrete before cracks develop. The rapid response, namely core material dissolution and reaction product precipitation, can be realized after the rupture of capsules in presence of water, as shown in Fig. 2. In the alkaline liquid environment (pH > 7) of cement-based materials, the associated chemical reaction of the healing agents is shown in Eq. (1).

$$Ca(CH_3COO)_2 + Na_2CO_3 \xrightarrow{H_2O,\ OH^-} CaCO_3 + 2CH_3COONa \quad (1)$$

2. Materials and methods

2.1. Materials

Portland cement classified as PO.42.5 (Chinese company Hailuo) with a specific area of 0.37 cm^2/g and specific gravity of 3.1 g/cm^3 was used for mortar specimens. The chemical composition of cement determined by X-ray fluorescence spectrometry (ARL Perform' X 4200, Thermo Fisher, America) was listed in Table 1. ISO standard sand provided by Xiamen ISO standard sand Co., Ltd was used for mortar specimens.

PEG (Sinopharm Chemical Reagent Co., Ltd) with an average molecular weight of 1000 and melting temperature of approximately 37 °C, calcium acetate ($Ca(CH_3COO)_2$, Shanghai Titan Scientific Co., Ltd) and sodium carbonate (Na_2CO_3, Shanghai Titan Scientific Co., Ltd) were used as core materials of the capsules. Epoxy resin and hardener (M02 type, Kunshan chemical company) was designed with an epoxy resin to hardener ratio of 10 : 3. The epoxy mixture has a viscosity of 700–1100 mPas, curing time of 3–4 h (25 °C), and a operating time of 20–30 min. River sand with a size of 0.15–0.3 mm was applied on the coating of capsules to improve bond between the capsules and cementitious matrix.

2.2 Capsules preparation.

This study developed three types of capsules as self-healing agents for cement-based materials (Table 2). Based on the core materials, the capsules can be denoted as CA (calcium acetate), SC (sodium carbonate), and CC (composite core materials including calcium acetate and sodium carbonate). Among them, capsules CA and SC should be utilized together, forming a double-capsule healing system, while capsule CC was applied to the cement matrix alone (single-capsule healing system). In all three capsules, PEG was introduced to bind the loose crystal powders together without affecting their physicochemical properties. SAP was incorporated in those capsules. The influence of SAP on self-healing efficiency of the capsules was also investigated.

In this study, a modified manufacturing method of capsules according to the previous study was used [36]. The preparation process of the capsules was as follows. The pelletization process was similar to the method in the study aforementioned, but the difference lay in the composition and structure of wall materials.

- Pelletization process:

Firstly, the crystal powders (i.e., calcium acetate and sodium carbonate) and PEG (according to the ratio of Table 2) were preheated to 40 °C. The powders were stirred at a low speed for 30 s in a mortar mixer, then PEG liquid was added into the mixture and stirred at a low speed for 60 s, then at high speed for 120 s. After mixing, the core material was cast on a plate and placed at 20 °C, RH = 40% environment for hardening. After 6 h, the hardened core materials were crushed, and the particles with a size of 2.36–4.75 mm were sieved out for further treatment.

- Coating process:

(a) Coating of a sand layer:

The particles obtained from the pelletization process were mixed with small amount (according to the ratio of Table 2) of epoxy mixture

Table 4
Mix design of mortar.

Code	Mix description	Cement (g)	Sand (g)	Water (g)	Capsule (g)
PC	Plain mortar as control	450	1350	225	–
DC	Mortar incorporated SC-A and CA-A (double-capsule healing system, composite-wall structure, without SAP)	450	1209.45	225	CA-A: 52 SC-A: 37
DDS	Mortar incorporated SC-B and CA-B (double-capsule healing system, double-wall structure, with SAP)	450	1209.45	225	CA-B: 52 SC-B: 37
SCS	Mortar incorporated CC-C (single-capsule healing system, composite-wall structure, with SAP)	450	1209.45	225	CC-C: 88.5
DCS	Mortar incorporated SC-C and CA-C (double-capsule healing system, composite-wall structure, with SAP)	450	1209.45	225	CA-C: 52 SC-C: 37

for 5 min. After standing for about 0.5 h, the particles coated with epoxy resin were mixed with fine sand in a coating machine at a speed of 45 r/min for 10–15 s. Note that the sand also plays a role in separating the particles coated with epoxy resin. After 12-h hardening of epoxy resin, capsules with a 2.36–4.75 mm diameter were sieved out and stored under 40% relative humidity 20 °C.

(b) Coating of a pure epoxy resin layer: The particles obtained from step (a) were mixed with the epoxy mixture for 5 min to ensure the even distribution of epoxy on the surface of the particles. Those particles were then separated from each other to wait for the solidification of epoxy, forming a waterproof shell around the particles.
(c) Another coating of a sand layer

Presumably, the structure of wall materials has a great influence on the healing effect and efficiency of those capsules for self-healing concrete. Therefore, three types of capsules, as shown in Table 3, were fabricated for further experimental research. A-type capsules (CA-A, SC-A, and CC-A) represented those without SAP but with a composite-wall structure prepared through steps (a), (b), and (c). B-type capsules (CA-B, SC-B, and CC-B) represented those with SAP and with a double-wall structure fabricated merely through steps (a) and (c). Another epoxy resin layer was introduced by applying step (b) to B-type capsules to obtain the C-type ones (CA-C, SC-C, and CC-C).

2.2. Waterproof property and alkali resistance of wall materials

In the process of cement hydration, the maximum pH value of cement paste can reach about 13 [37]. Hence, the sodium hydroxide solution (pH ≈ 13) was prepared to simulate the pore solution of Portland cement paste. Then the capsules (CA-B, SC-B, CC-B, CA-C, SC-C, and CC-C type) were submerged in the sodium hydroxide solution, and the conductivity of the supernatant liquid was tested to evaluate the

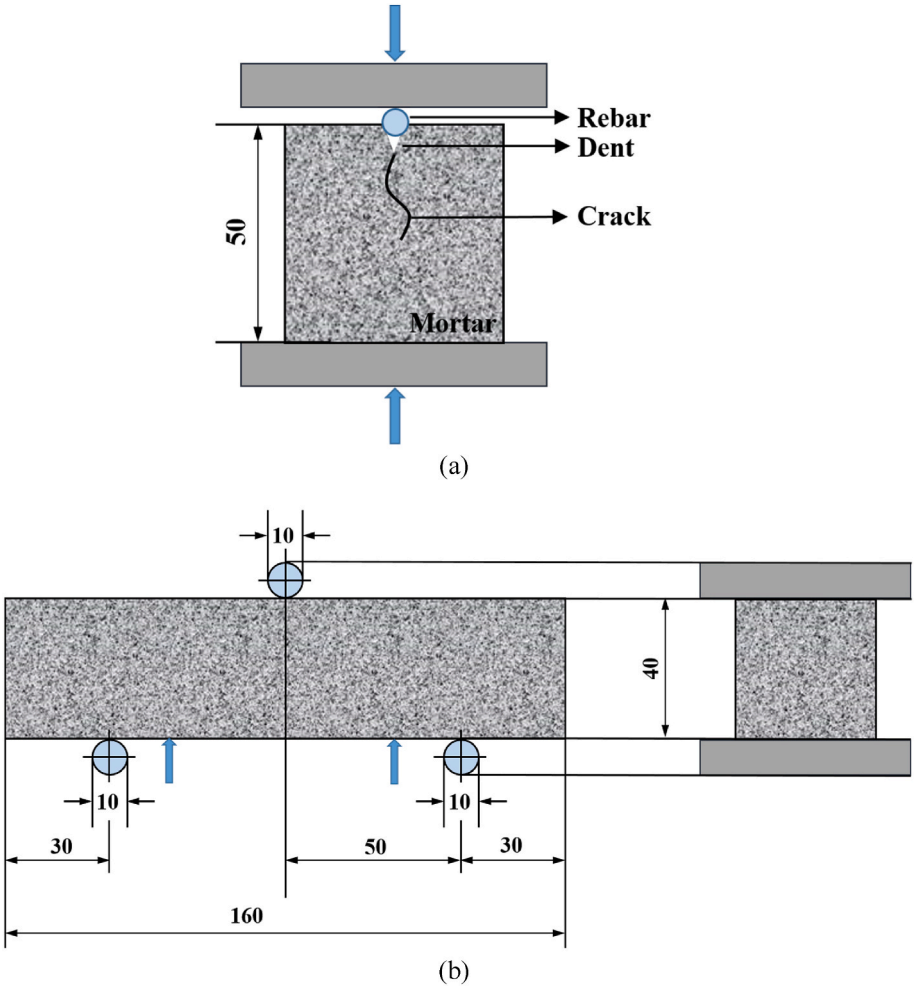

Fig. 3. A schematic of the test set-up for crack fabrication: (a) splitting; (b) flexural test.

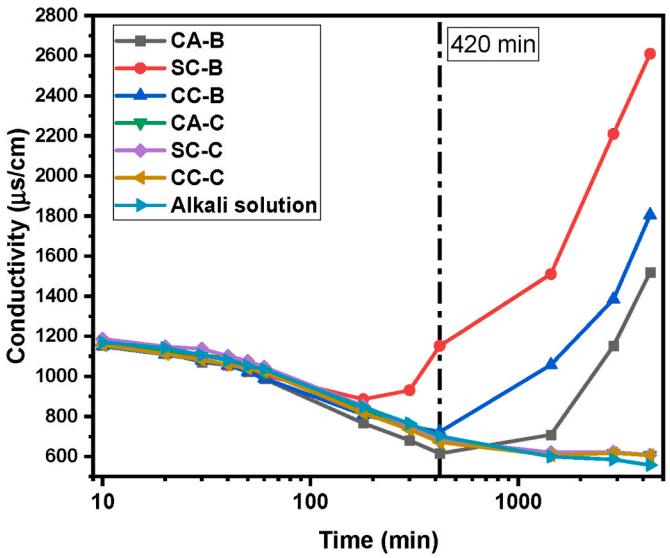

Fig. 4. Electrical conductivity of suspensions of solution with different types of capsules.

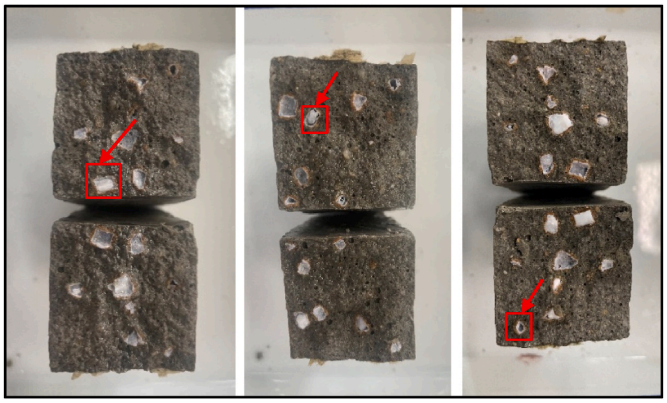

Fig. 5. Fracture section diagram of CA-B capsule mortar specimens.

waterproof efficiency of the different wall materials with a liquid to solid mass ratio of 20. A conductivity meter (DDS-11A, Lighting, China) was used to measure the conductivity of the supernatant liquid after the capsules were submerged in the solution for 10 min, 20 min, 30 min, 40 min, 50 min, 60 min, 3 h, 5 h, 7 h, 1 day, 2 days, 3 days, 5 days and 7 days.

2.3. Mortar specimen preparation and crack fabrication

Five series of specimens with the ratio of cement: sand: water was 1: 3: 0.5 were made and the mix design of mortar is listed in Table 4. Except for the group PC, the capsules were incorporated as a partial substitution of sand at 6% by mass for all groups. According to Chinese standard GBT 17671-1999, water and cement were mixed for 30 s at a low speed. Then, the sand and capsules were added and continuously mixed for 30 s at a high speed. After pausing for 90 s, the mortar was mixed for another 60 s at a high speed. Afterwards, the mortar was cast into cubic molds (50 mm × 50 mm × 50 mm) for the X-ray CT test and prism molds (40 mm × 40 mm × 160 mm) for the X-ray CT test and water permeability test. The specimens were demolded after 24 h and cured in a curing room (20 ± 2 °C, RH ≥ 95%).

After 7 days of curing, the cubic specimens were pre-cracked by splitting as shown in Fig. 3(a). The dent above the cube was made by cutting for controlling crack propagation. The prism specimens were subjected to a flexural test to create cracks (Fig. 3(b)). The loading rate of the bending machine was 25 N/s to control the crack width. Before the flexural test, four sides of prisms were wrapped with tape along the long axis of prisms to keep their integrity. Then the five groups of mortar specimens were immersed in water separately at room temperature for healing.

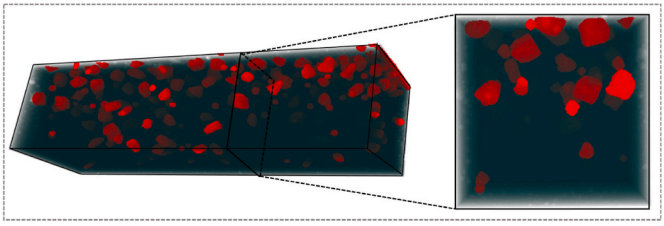

Fig. 7. Distribution of capsules in mortar matrix (capsules are shown in red). (For interpretation of the references to colour in this figure legend, the reader is referred to the Web version of this article.)

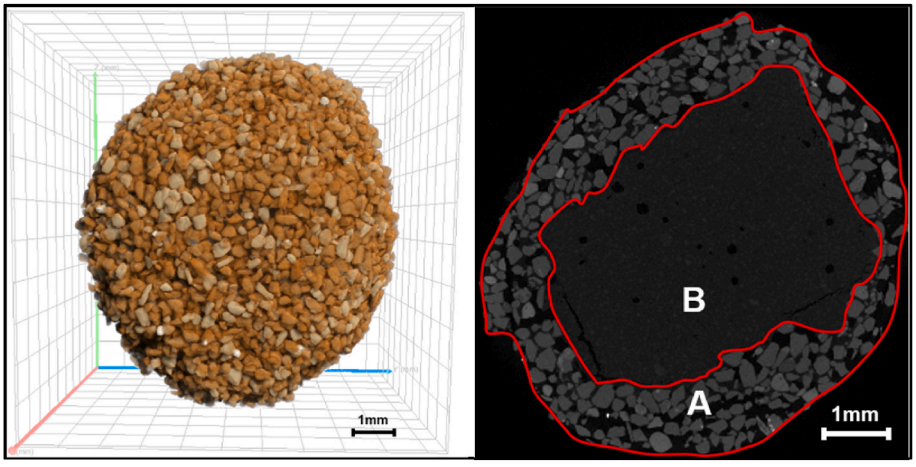

Fig. 6. Nano-CT images of the CC-C type capsule. (a): The 3D image of the capsule; (b): The 2D image of the internal structure of the capsule (A: wall material; B: Core material).

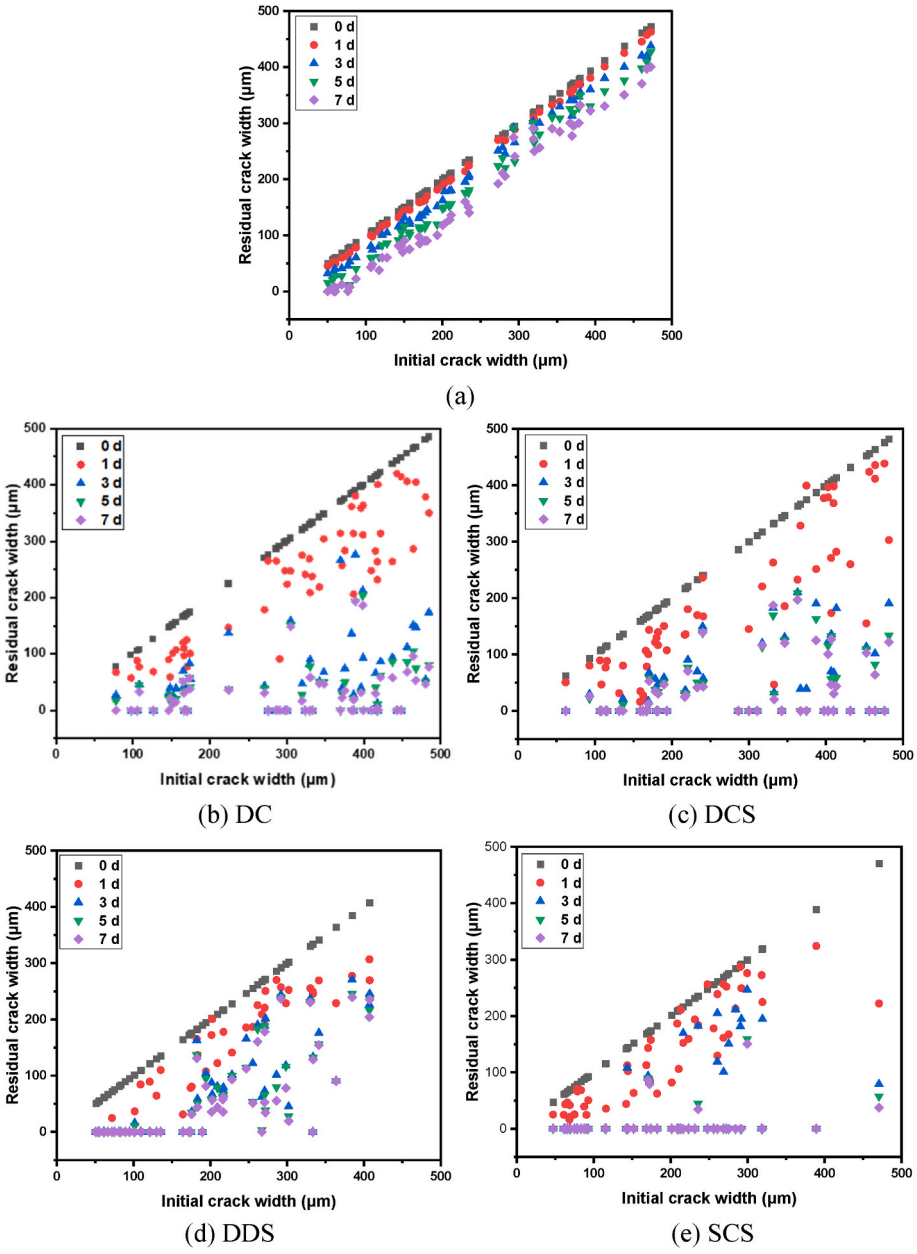

Fig. 8. Crack width analysis.

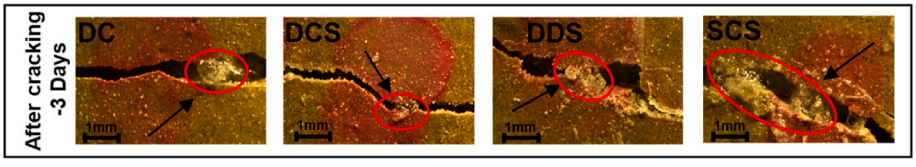

Fig. 9. The image of crack surface with SAP.

2.4. Structure of the capsule and distribution in mortar matrix

The 3D X-ray microscope (Xradia 510 Versa, Zeiss) (60× kV scanning voltage, 0.4 × objective, 8.17 μm resolutions) was used for observing the structure of capsules (CC–C type), and to estimate the volume ratio of the core material to the wall material. The 3D images were reconstructed and analyzed with ORS Dragonfly software (ver.2020.02, Canada). The morphology of capsules was observed by using a stereomicroscope. To detect the distribution of capsules in mortar matrix, the uncracked prism specimens obtained from section 2.5 were subjected to X-ray CT test (195 kV scanning voltage, 0.19 mA current).

2.5. Evaluation of the self-healing effect

2.5.1. Visualization of crack filling

A stereo microscope with Mshot software was utilized to observe and measure the surface crack width before and after healing. The cubic specimens of different groups were submerged separately throughout

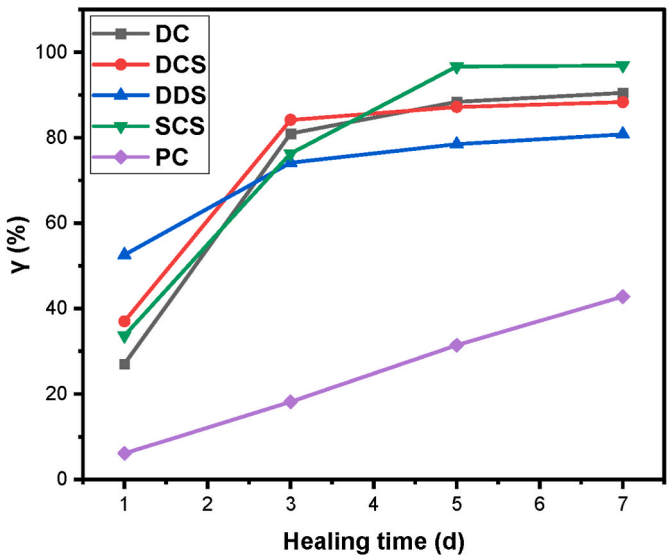

Fig. 10. Average sealing ratio over time for each mix.

the entire healing stage. Nine sites on each crack in the specimens were selected for measurements before healing and after healing for 1 day, 3 days, 5 days, and 7 days. The distance between each site was about 3 mm. The sealing efficiency was calculated with the following equation:

$$\gamma = \frac{W_i - W_t}{W_i} \times 100\% \quad (2)$$

where γ is the sealing ratio [%]; W_i is the initial crack width [μm]; W_t is the crack width after healing for t days [μm].

Furthermore, the interior of cracks of cubic specimens in group DCS after 1 day healing was measured by performing X-ray CT test (195 kV scanning voltage, 0.19 mA current). The ORS Dragonfly software (ver.2020.02, Canada) was used to reconstruct 3D images of cubic specimens.

2.5.2. Permeability of cracked specimens

Water permeability test was conducted on pre-cracked prism specimens using modified equipment described in RILEM method No. II. 4 [38]. The water head was 100 cm from the upper surface crack. Before the measurements, the lateral sides of specimens were sealed by paraffin. An electronic balance was used to measure the mass of water penetrating through mortar crack after. The testing duration was 10 min for each specimen with a healing time of 0 day, 1 day, 3 days, 5 days, and 7 days. After each test, the prism specimens were immersed in water for further healing. Referring to the methods of Zhengwu Jiang [39] and E. Tziviloglou [40], the recovery ratio of water tightness (RWT) was used to characterize the improvement of impermeability of specimens after repair with the following equation:

$$RWT = \frac{W_{n-h(t)} - W_{h(t)}}{W_{n-h(t)}} \quad (3)$$

Where $\boldsymbol{RWT}$ is the recovery ratio of water tightness [%]; $\boldsymbol{W_{n\text{-}h(t)}}$ is the average mass of water penetrating through the unhealed cracks of three specimens [g]; $\boldsymbol{W_{h(t)}}$ is the average mass of water penetrating through the cracks of three specimens after healing [g]; $\boldsymbol{t}$ is the healing time [day].

2.5.3. Analysis of self-healing products

After healing for 7 days, the fragments of group DC, SCS, and DCS were obtained by cutting. The microstructure of healing products was investigated by scanning electron microscope (SEM, FEI 3D, America) equipped with energy dispersive spectroscopy (EDS). To avoid any influence of immersion in absolute ethyl alcohol on SAP morphology, all the samples were only dried in a freezer dryer for 48 h.

The x-ray diffraction (XRD) analysis was conducted using a D8 automatic XRD equipped with Cu Ka radiation (30 kV and 30 mA, scan

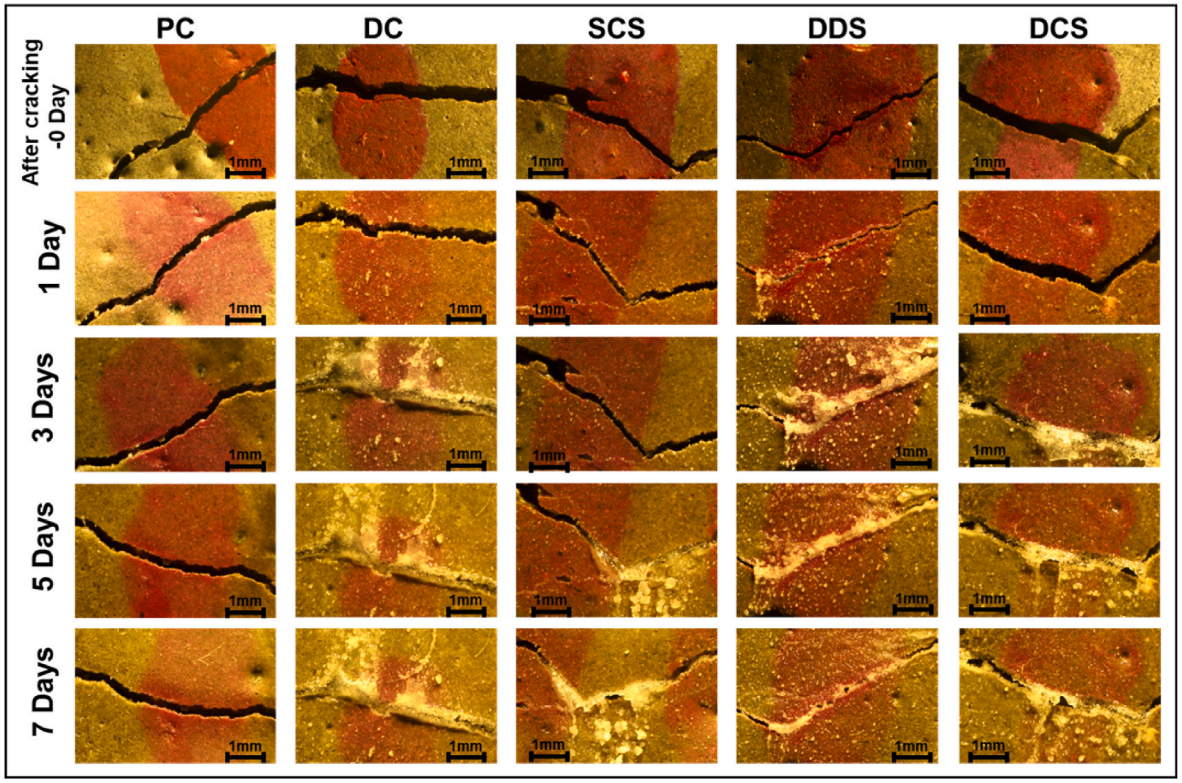

Fig. 11. Representative image of efficient crack sealing patterns over time for each mix.

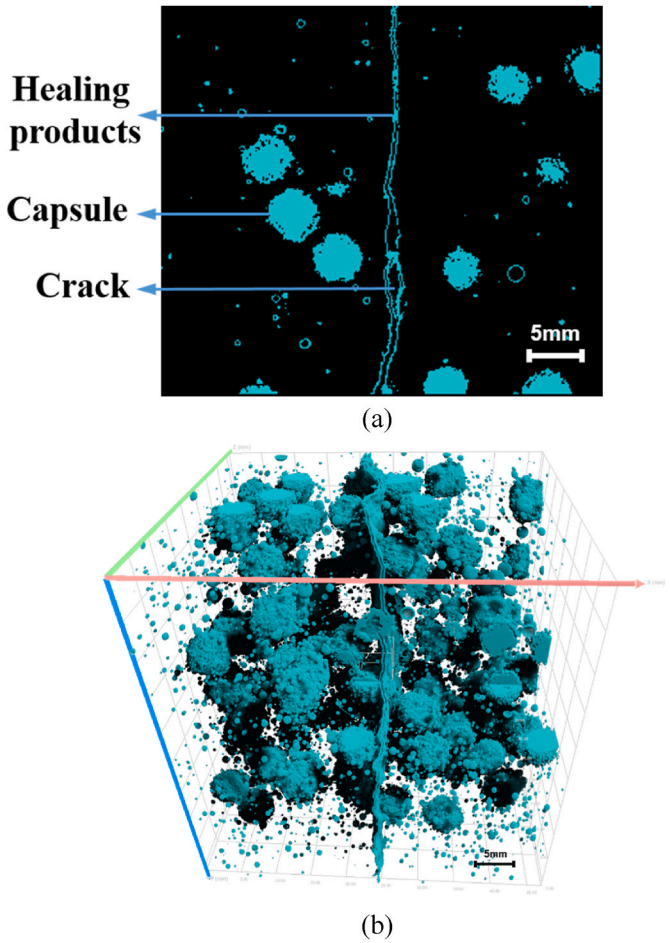

Fig. 12. X-CT image of crack interior of cubic specimens in group DCS. (a): The 2D image of the cubic specimen interior; (b): The 3D image of internal structure of cubic specimen.

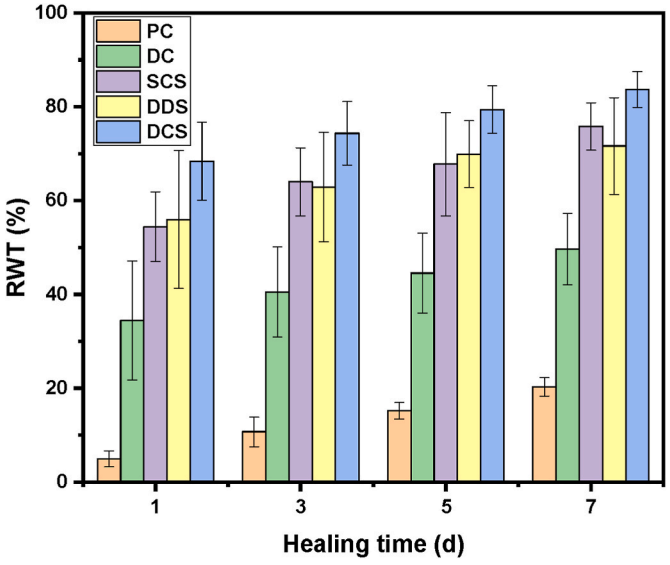

Fig. 13. Average recovery rates of water tightness values.

interval 5–70° (2 theta), 0.02° and 0.15 s per step) to determine the composition of healing products. After healing for 7 days, the cracked specimen was placed into a beaker filled with water and the white precipitate attached to the fracture surface was obtained by using an ultrasonic cleaner, following the method used in Ref. [41]. The samples for the XRD test were dried in a vacuum oven at 60 °C for 48 h. They were ground, and particles smaller than 75 μm were obtained by sieving.

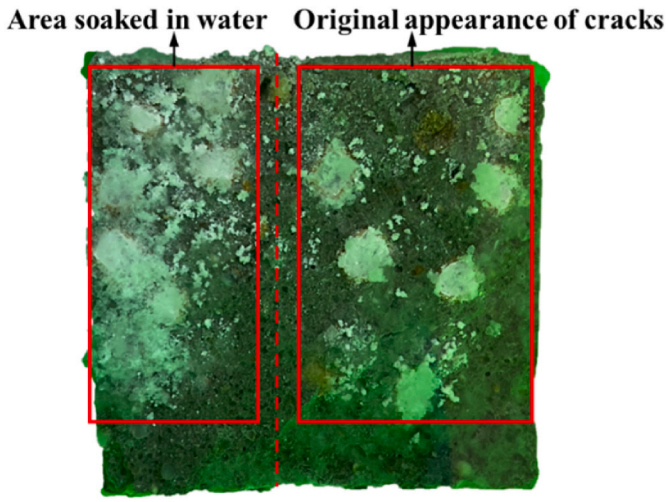

Fig. 14. The comparison between the original appearance of cracks after healing for 1 d and the area soaked in water for another 1 h (SCS specimen).

3. Results and discussion

3.1. Waterproof property and alkali resistance of wall materials

The conductivity of the supernatant liquid is shown in Fig. 4. Within 420 min, the conductivity curves of all group of the capsules were basically the same as the reference solution (i.e., alkali solution), indicating that the wall material with a certain thickness could effectively resist the erosion of alkaline solution during this period. However, the conductivity curves of CA-B, SC-B, CC-B (double-wall structure) suddenly increased significantly at 1 day and kept increasing afterwards. Sodium carbonate and calcium acetate in the core material are soluble substances, which could release sodium ions, carbonate ions, and calcium ions, and significantly improve the conductivity of the solution. Therefore, it can be inferred that the double-wall structure was capable of preventing lye erosion to a certain extend. However, as the immersion time increased, the solution entered the interior of the capsule driven by the capillary force formed in the interfacial gap between epoxy resin and sand. This was further proved in the mortar specimens. Fig. 5 shows the rupture surface of the specimens incorporated with CA-B capsules cured for 3 days, and the core material of the capsule has partially dissolved. Hence, the double-wall structure cannot effectively guarantee the repair potential of self-healing capsules. In contrast, the conductivity curves of the other three groups (CA-C, SC-C, and CC-C (composite-wall structure)) were consistent with the reference solution, indicating that the sodium carbonate and calcium acetate in the core material were effectively protected by encapsulation. Hence, compared to the double-wall structure, the composite-wall structure endowed the capsules with excellent waterproof efficiency and alkali resistance due to the pure epoxy resin layer that enhanced the protection of core materials against alkali solution.

3.2. Structure and distribution of the capsule

Each coating layer of the capsules was designed for different purposes. The inner sand layer was aimed to improve the strength of the wall material to avoid the rupture of the capsule when mixing mortar mixtures; the middle epoxy resin layer was to improve the waterproof and alkali resistance of the wall material to maintain the repair potential of core material; the outermost sand layer was designed to increase the

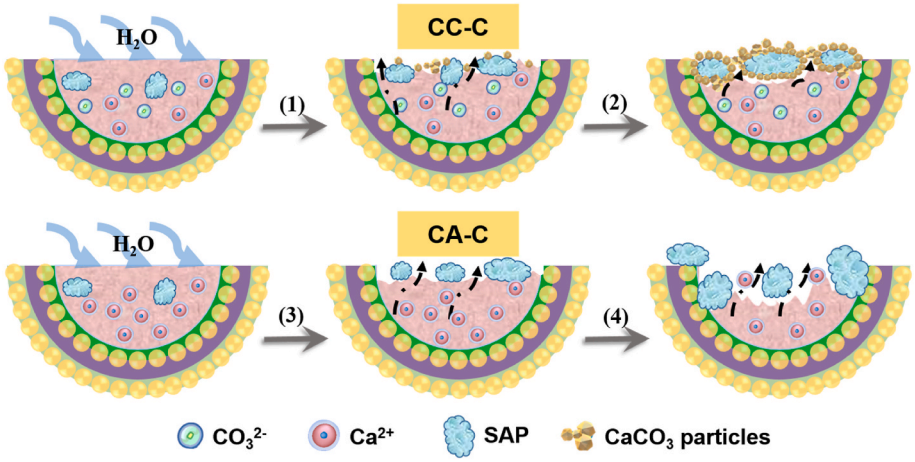

Fig. 15. Schematic illustration of early healing process of the single-capsule healing system (take CC-C capsule for example) and double-capsule healing system (take CA-C capsule for example). The single-capsule healing system: (1) The surface dissolution of core material, partial precipitation of $CaCO_3$ particles; (2) The SAP wrapped in $CaCO_3$ particles hinders the dissolution of the core materials. The double-capsule healing system: (3–4) The dissolution of core materials and SAP swelling process is carried out smoothly in the early stage.

roughness and thus increase the bonding force between the capsules and the cement matrix to improve the cracking efficiency of the capsule when cracks occurred [7]. Fig. 6(a) shows the CC-C type capsule with a rough surface, and Fig. 6(b) shows the internal structure of the capsules. The thickness of the wall material was about 400–1000 μm. Note that the epoxy resin layer cannot be clearly distinguished between the two sand layers in the figures, explained by the fact that the epoxy resin filled the uneven surface of the first sand layer when the pure epoxy resin layer was introduced.

The distribution of capsules in the mortar matrix is shown in Fig. 7. It can be found that the capsules were evenly distributed horizontally inside the mortar matrix. However, few capsules were distributed in the lower part of the specimen and the capsules appeared to float up. As a matter of fact, the apparent density of the several types of capsules was similar, about 1685 kg/m^3. In contrast to that of cement mortar, more than 1900 kg/m^3, the capsules had lower apparent density and tended to float up during vibration. In essence, the capsules belong to lightweight aggregates. In engineering, a proper distribution of lightweight aggregate can be ensured by increasing the viscosity of mortar [42], increasing the stirring time, and adopting the pressure vibration molding technology [43], while this is out of the scope of this study.

3.3. Evaluation of the self-healing effect

3.3.1. Visualization of crack filling

The reduction of crack width over the healing time is demonstrated in Fig. 8(a–e) for each mix. The initial crack width was between 50 and 500 μm. In this study, the change in crack width was used to evaluate the efficiency of self-healing. It was observed that the PC specimens has only limited self-healing capacity, since the crack width was basically unchanged after healing for 1 day and the crack smaller than 100 μm has been closed after healing till 7 days. For the other mixtures, the crack width up to about 200 μm has been basically sealed within 3 days. In general, after 7 days of healing, both large and small cracks presented satisfactory self-healing effects and the vast majority of cracks were sealed completely. Therefore, the specimens incorporating the capsules developed in this paper showed high self-healing efficiency compared to other capsule-based self-healing techniques, which usually require longer time to seal the crack [28,36]. In addition, for specimens incorporated with capsules, some crack widths from 50 to 300 μm suddenly decreased to 0 μm, possibly due to long observation intervals, which also proved the rapidity of the capsules healing. Some SAP was observed in the crack surface (Fig. 9), showing that the SAP in core materials could migrate in cracks.

The average sealing ratio was shown in Fig. 10. Overall, the average sealing ratio showed a drastic increase after healing for 3 days, indicating that the functional components could be effectively released within 3 days. Based on the analysis of crack width, it was found that the trend of average sealing ratio of DC and DCS specimens over the healing time was similar. The average sealing ratio of SCS specimens was the highest among all five mixtures, up to 96% after healing for 7 days. This can be explained by the smaller widths (mostly below 300 μm) of cracks in SCS specimens, which were easier to heal (see Fig. 8(e)). In contrast, the average sealing ratio of DDS specimens was the highest after healing for 1 day, but the lowest ultimately. This may be explained by the fact that compared with the composite-wall structure, the double-wall structure has poor waterproof property (Fig. 4) and the core material has partially dissolved into the pores around the capsules (Fig. 5). Therefore, when the cracked specimens were immersed in water, the core dissolution and migration in DDS was triggered faster compared with other groups. However, part of the dissolved functional components may be consumed during cement hydration process, resulting in low sealing efficiency in later period.

The representative images of efficient crack sealing patterns over time for each mix were shown in Fig. 11. The crack surface of the PC control group was almost unchanged, but the cracks in other group were all sealed in the end. In addition, the healing products on the surface of the crack were loose, and the friction during the photographing caused some damage to the healing products. This was plausible, because the healing products were obtained by chemical deposition, and did not develop high mechanical properties.

The reconstructed 3D image of the DCS specimen is shown in Fig. 12. The capsules in uncracked areas were intact. It indicates that the capsule with a composite-wall structure had sufficient mechanical properties against the mixing process of mortar mixtures which would cause premature rupture of capsules. Furthermore, the healing product was uniformly deposited on the fracture surface. It is worth noting that due to the low resolution of X-CT, CT images can only show the position and morphology of the bulk healing product, but cannot accurately quantify the volume of the product. Moreover, the SAP and calcium carbonate cannot be easily distinguished accurately by the technique used in this study.

3.3.2. Permeability of cracked specimens

The recovery ratio of water tightness (RWT) was shown in Fig. 13. For PC specimens, the water tightness recovery ratio at 1 day was about 5%, and increased to approximately 20% after autogenous healing for 7 days, which is similar to the results in previous study [36]. In contrast, the RWT of specimens incorporated with capsules was much higher than that of PC specimens. The RWT of DC specimens was 34% after healing for 1 day, followed by minor improvement in the next 6 days. The RWT of SCS and DDS specimens showed similar results, which was about 55% after healing for 1 day and increased to 75% at 7 days. The RWT of DCS specimens was the highest among them, which achieved 68% at 1 day to

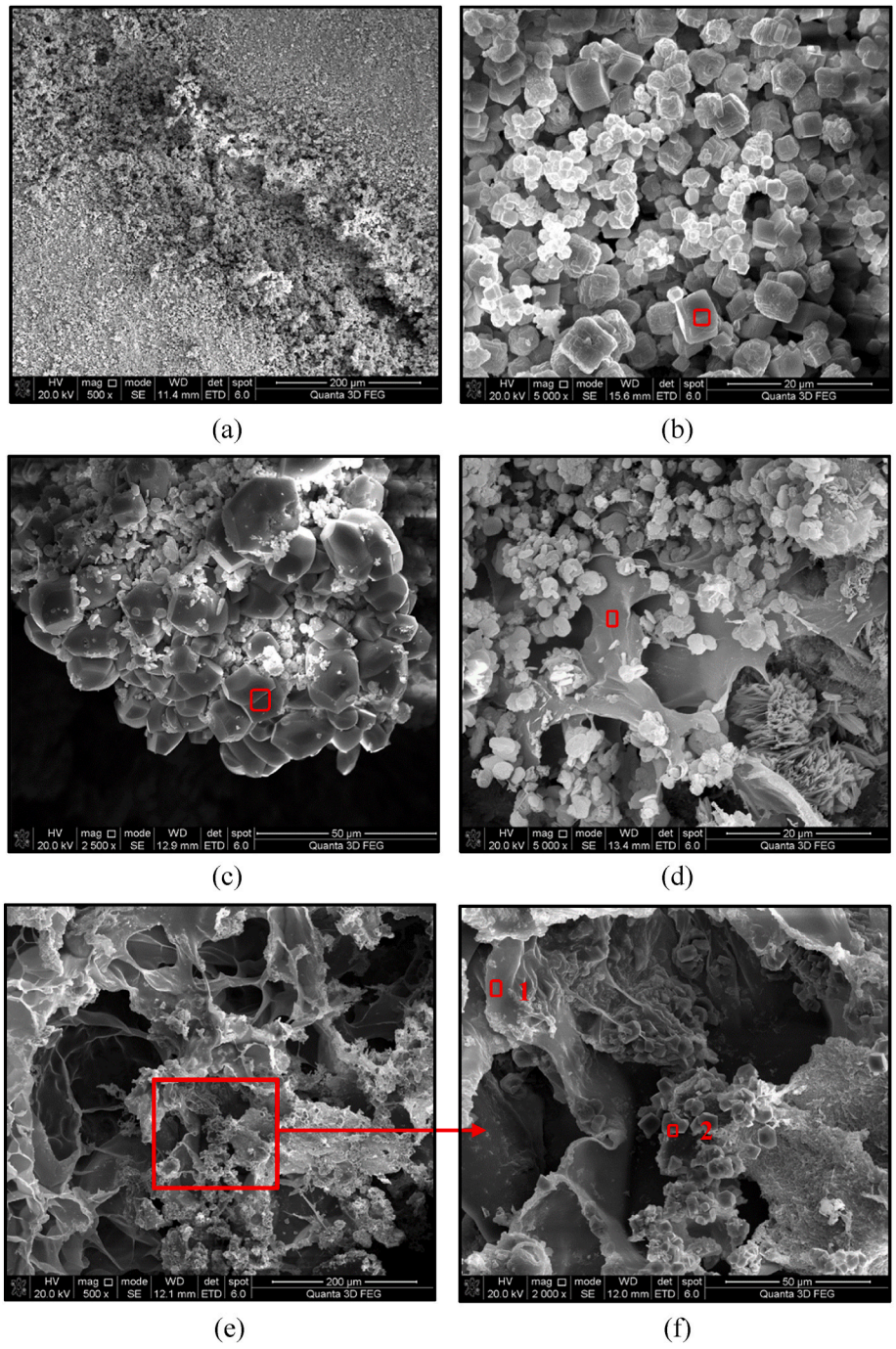

Fig. 16. After healing for 1 d, (a) SEM image of the crack surface being sealed of DC specimens; (b) SEM image of precipitation inside the crack of DC specimens; (c) SEM image of SAP surface covered by precipitation inside SCS specimens; (d) SEM image of precipitation inside SAP of SCS specimens; (e–f) SEM image of healing product inside the crack of DCS specimens.

Table 5
Element composition of the selected region in SEM images of Fig. 15.

Region	C (Atomic %)	O (Atomic %)	Ca (Atomic %)	Si (Atomic %)
b	20.1	58.6	21.3	–
c	16.1	61.1	22.8	–
d	14.8	83.0	2.1	0.1
f-1	41.0	56.0	1.8	–
f-2	24.2	65.1	20.7	–

84% at 7 days. Hence, after incorporating the capsules, the permeability of cracked specimens reduced tremendously within a short time compared to the previous study [28]. Moreover, comparing DC with DCS specimens, it was found that the incorporation of SAP in the core materials of capsules can significantly improve the water tightness of cracked specimens after healing, which is consistent to the findings in literature [44,45]. Compared with SCS, DCS specimens, the double-capsule system has a higher water tightness recovery ratio, indicating that the products of the double-capsule system were more evenly distributed in the cracks. The RWT gap between DDS and DCS specimens further verified that the composite-wall structure has better waterproof property and alkali resistance. SAP played a vital role in the

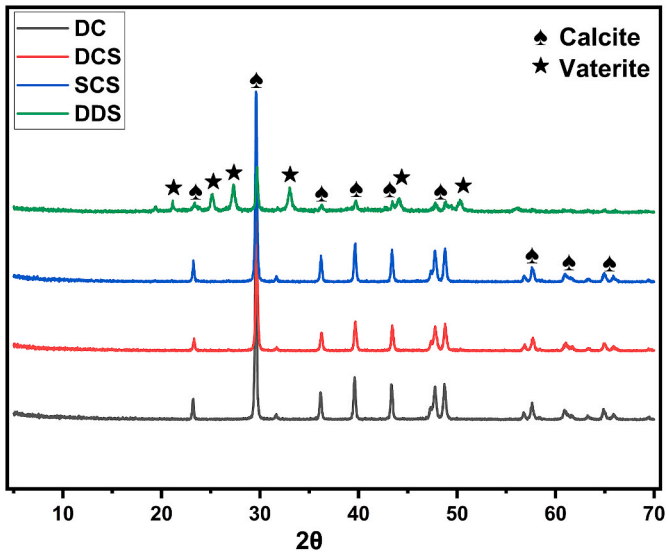

Fig. 17. XRD pattern of the self-healing product.

plugging of the crack interior from this session. The recovery can be ranked in this order DCS > SCS = DDS > DC > PC. Therefore, it could be concluded that capsules developed in this study could realize fast response and healing effect for cracked mortar specimens submerged in water.

In particular, difference in RWT between SCS and DCS specimens was about 8% since the core materials of SCS contained both sodium carbonate and calcium acetate, causing precipitation immediately after submersion in water. The generated micron-sized calcium carbonate was attached to the surface of SAP (Fig. 16(c–d)) on the surface of the core materials, hindering the contact with water. Therefore, in the interior parts of the capsules, the dissolution of ions, precipitation of calcium carbonates and water absorption of SAP were hindered. This explanation can be supported by the comparison between the original appearance of cracks after healing for 1 day and the area submerged in water for another 1 h (SCS specimen) as shown in Fig. 14. In contrast, since the functional components of DCS specimens were encapsulated in two types of capsules, the dissolution of core materials and SAP swelling process took place smoothly in the early stage, resulting in a better RWT. The schematic illustration of early healing process of the single-capsule healing system (take CC-C capsule for example) and double-capsule healing system (take CA-C capsule for example) was shown in Fig. 15.

3.3.3. *Analysis of self-healing products*

The SEM images of crack surface and interior of DC, SCS, and DCS specimens were shown in Fig. 16. Fig. 16(a) shows that the crack could be sealed completely by products. Fig. 16(b) shows the morphology of healing products around the capsule inside the crack of DC specimens after healing for 1 day. Healing products mainly had a cubic structure and partially had a spherical structure with particle sizes ranging from 1 to 7 μm. It could be confirmed by EDS (Table 5) that the products were calcium carbonate. The signs of crystal growth and mutual cementation between the healing products could be seen in Fig. 16(b). As shown in Fig. 16(c–d), for SCS specimens, SAP was not only tightly wrapped by precipitates, but also has a large amount of calcium carbonate in the internal pores, which hindered the swelling of SAP. It has been reported that Ca^{2+} in the solution can bind with carboxylate groups in the acrylate chains of SAP, forming additional cross-links [46]. Although the swelling of SAP was inhibited, the cross-links between SAP and calcium ions can enhance the adhesion between calcium carbonate and SAP and improve the stability of the repair products. For DCS specimens (Fig. 16(e–f)), the main elements of cubic precipitating inside the SAP were C, O, and Ca, indicating that the precipitates were $CaCO_3$. The three-dimension crosslinked network was SAP with main elements of C and O.

To determine the difference in the composition of healing produts among all mixtures, the white precipitate was collected and analyzed. Fig. 17 shows the XRD results for each mix, it was found that the healing products of each mix were calcium carbonate, which existed in the form of calcite and vaterite. Furthermore, the calcite phase was found in DC, SCS, DDS, and DCS samples. Unlike SCS, DC, and DCS samples, the vaterite phase was identified at peaks of 25°, 27°, 33°, 44° and 50° in the DDS sample. From the previous study, the calcite phase is preferable in terms of stability [47].

4. Conclusions

In this study, a fast-responsive self-healing technology based on capsules is developed with sodium carbonate (Na_2CO_3) and calcium acetate ($Ca(CH_3COO)_2$) as healing agents. Poly (ethylene glycol) (PEG), a phase change material, is used for granulation of the healing agents. The composite-wall structure is composed of a sand layer, a pure epoxy resin layer and another sand layer. For the purpose of determining the structure of the capsules and distribution in the matrix, the Nano-CT and X-CT test were performed, respectively. Furthermore, the waterproof efficiency and alkali resistance of different wall materials were investigated through electrical conductivity. Ultimately, the self-healing efficiency of mortars incorporated capsules was evaluated by analyzing the crack width, average sealing ratio, and water tightness recovery rates. The SEM and XRD were used to observe the morphology and phases of healing products. The conclusions of this study were summarized as follows:

1. The waterproof property and alkali resistance of composite-wall structure was superior to double-wall structure. The introduction of a pure epoxy resin layer could significantly enhance the waterproof property of the capsules.
2. It was identified that the sealing of crack surface was attributed to the formation of calcium carbonate. In general, after 7 days of healing, both large and small cracks exhibited a satisfactory sealing effect and the vast majority of cracks were sealed completely for specimens with capsules.
3. SAP played a vital role in the plugging of the crack interior. Incorporation of the capsules with SAP could drastically increase recovery rates of water tightness of cracked specimens. The recovery ratio of water tightness of DCS specimens was the highest among them, which had an RWT from 68% at 1 day to 84% at 7 days.
4. Healing products had particle sizes ranging from 1 to 7 μm mainly with a cubic structure and partially with a spherical structure. The healing products of each mix were calcium carbonate, which existed in the form of calcite and vaterite.

Author contributions

The authors declare that they have no known competing financial interests or personal relationships that could have appeared to influence the work reported in this paper. The corresponding author is responsible for ensuring that the descriptions are accurate and agreed by all authors. Corresponding author: Ruixing Wang, Hua Dong Main contributions: Advice, evaluation, and successful completion of coaching papers. Acquisition of the financial support for the project leading to this publication. Jian Gao: Main contributions: Ideas; formulation or evolution of overarching research goals and aims. Development or design of methodology; creation of models. Conducting a research and investigation process, specifically performing the experiments, or data/evidence collection. Peng Jin, Yuze Zhang: Main contributions: Auxiliary experimental tests. Recommendations and comments.

Declaration of competing interest

The authors declare that they have no known competing financial interests or personal relationships that could have appeared to influence the work reported in this paper.

Data availability

Data will be made available on request.

Acknowledgements

The authors would like to acknowledge financial support from the National Natural Science Foundation of China (51872046); and the Natural Science Foundation of Jiangsu Province, China (BK20191270).

References

[1] C.M. Aldea, S.P. Shah, A. Karr, Permeability of cracked concrete, Mater. Struct. 32 (5) (1999) 370–376.
[2] L. Basheer, J. Kropp, D.J. Cleland, Assessment of the durability of concrete from its permeation properties: a review, Construct. Build. Mater. 15 (2–3) (2001) 93–103.
[3] H.-W. Reinhardt, M. Jooss, Permeability and self-healing of cracked concrete as a function of temperature and crack width, Cement Concr. Res. 33 (7) (2003) 981–985.
[4] K. Wang, D.C. Jansen, S.P. Shah, A.F. Karr, Permeability study of cracked concrete, Cement Concr. Res. 27 (3) (1997) 381–393.
[5] X.F. Wang, Z.H. Yang, C. Fang, N.X. Han, G.M. Zhu, J.N. Tang, F. Xing, Evaluation of the mechanical performance recovery of self-healing cementitious materials – its methods and future development: a review, Construct. Build. Mater. 212 (2019) 400–421.
[6] C. Edvardsen, Water permeability and autogenous healing of cracks in concrete, ACI Mater. J. 96 (4) (1999) 448–454.
[7] H. Huang, G. Ye, C. Qian, E. Schlangen, Self-healing in cementitious materials: materials, methods and service conditions, Mater. Des. 92 (2016) 499–511.
[8] E. Schlangen, C. Joseph, Self-Healing Processes in Concrete, 2009, pp. 141–182.
[9] S. Granger, A. Loukili, G. Pijaudier-Cabot, G. Chanvillard, Experimental characterization of the self-healing of cracks in an ultra high performance cementitious material: mechanical tests and acoustic emission analysis, Cement Concr. Res. 37 (4) (2007) 519–527.
[10] J.Y. Wang, H. Soens, W. Verstraete, N. De Belie, Self-healing concrete by use of microencapsulated bacterial spores, Cement Concr. Res. 56 (2014) 139–152.
[11] K. Van Tittelboom, N. De Belie, W. De Muynck, W. Verstraete, Use of bacteria to repair cracks in concrete, Cement Concr. Res. 40 (1) (2010) 157–166.
[12] B. Park, Y.C. Choi, Self-healing capability of cementitious materials with crystalline admixtures and super absorbent polymers (SAPs), Construct. Build. Mater. 189 (2018) 1054–1066.
[13] Z.-X. Hu, X.-M. Hu, W.-M. Cheng, Y.-Y. Zhao, M.-Y. Wu, Performance optimization of one-component polyurethane healing agent for self-healing concrete, Construct. Build. Mater. 179 (2018) 151–159.
[14] J. Qiu, H.S. Tan, E.-H. Yang, Coupled effects of crack width, slag content, and conditioning alkalinity on autogenous healing of engineered cementitious composites, Cement Concr. Compos. 73 (2016) 203–212.
[15] A.D. Oliveira, O.D.M. Gomes, L. Ferrara, E.D.R. Fairbairn, R.D. Toledo, An overview of a twofold effect of crystalline admixtures in cement-based materials: from permeability-reducers to self-healing stimulators, J. Build. Eng. 41 (2021).
[16] P. Mirjafari, K. Asghari, N. Mahinpey, Investigating the application of enzyme carbonic anhydrase for CO2Sequestration purposes, Ind. Eng. Chem. Res. 46 (3) (2007) 921–926.
[17] J. Wang, A. Mignon, G. Trenson, S. Van Vlierberghe, N. Boon, N. De Belie, A chitosan based pH-responsive hydrogel for encapsulation of bacteria for self-sealing concrete, Cement Concr. Compos. 93 (2018) 309–322.
[18] S. Bhaskar, K.M. Anwar Hossain, M. Lachemi, G. Wolfaardt, M. Otini Kroukamp, Effect of self-healing on strength and durability of zeolite-immobilized bacterial cementitious mortar composites, Cement Concr. Compos. 82 (2017) 23–33.
[19] J.Y. Wang, J. Dewanckele, V. Cnudde, S. Van Vlierberghe, W. Verstraete, N. De Belie, X-ray computed tomography proof of bacterial-based self-healing in concrete, Cement Concr. Compos. 53 (2014) 289–304.
[20] M. Alazhari, T. Sharma, A. Heath, R. Cooper, K. Paine, Application of expanded perlite encapsulated bacteria and growth media for self-healing concrete, Construct. Build. Mater. 160 (2018) 610–619.
[21] A.T. Henk, M. Jonkers, Bacteria mediated remediation of concrete structures, in: 2nd International Symposium on Service Life Design for Infrastructures, Delft, The Netherlands, 2010, pp. 833–840.
[22] Z.B. Bundur, M.J. Kirisits, R.D. Ferron, Biomineralized cement-based materials: impact of inoculating vegetative bacterial cells on hydration and strength, Cement Concr. Res. 67 (2015) 237–245.
[23] F.F. Ataie, M.C.G. Juenger, S.C. Taylor-Lange, K.A. Riding, Comparison of the retarding mechanisms of zinc oxide and sucrose on cement hydration and interactions with supplementary cementitious materials, Cement Concr. Res. 72 (2015) 128–136.
[24] Z. Li, M. Wyrzykowski, H. Dong, J. Granja, M. Azenha, P. Lura, G. Ye, Internal curing by superabsorbent polymers in alkali-activated slag, Cement Concr. Res. 135 (2020).
[25] H.X.D. Lee, H.S. Wong, N.R. Buenfeld, Potential of superabsorbent polymer for self-sealing cracks in concrete, Adv. Appl. Ceram. 109 (5) (2010) 296–302.
[26] D. Snoeck, D. Schaubroeck, P. Dubruel, N. De Belie, Effect of high amounts of superabsorbent polymers and additional water on the workability, microstructure and strength of mortars with a water-to-cement ratio of 0.50, Construct. Build. Mater. 72 (2014) 148–157.
[27] D. Gardner, R. Lark, T. Jefferson, R. Davies, A survey on problems encountered in current concrete construction and the potential benefits of self-healing cementitious materials, Case Stud. Constr. Mater. 8 (2018) 238–247.
[28] T.S. Qureshi, A. Kanellopoulos, A. Al-Tabbaa, Encapsulation of expansive powder minerals within a concentric glass capsule system for self-healing concrete, Construct. Build. Mater. 121 (2016) 629–643.
[29] T.H. Ahn, T. Kishi, Crack self-healing behavior of cementitious composites incorporating various mineral admixtures, J. Adv. Concr. Technol. 8 (2) (2010) 171–186.
[30] X. Liu, Q. Li, B. Li, W. Chen, A high-efficiency self-healing cementitious material based on supramolecular hydrogels impregnated with phosphate and ammonium, Cement Concr. Res. 144 (2021).
[31] K. Sisomphon, O. Copuroglu, A. Fraaij, Application of encapsulated lightweight aggregate impregnated with sodium monofluorophosphate as a self-healing agent in blast furnace slag mortar, Heron 56 (1–2) (2011) 17–36.
[32] A. Kanellopoulos, T.S. Qureshi, A. Al-Tabbaa, Glass encapsulated minerals for self-healing in cement based composites, Construct. Build. Mater. 98 (2015) 780–791.
[33] B.Q. Dong, Y.S. Wang, G.H. Fang, N.X. Han, F. Xing, Y.Y. Lu, Smart releasing behavior of a chemical self-healing microcapsule in the stimulated concrete pore solution, Cement Concr. Compos. 56 (2015) 46–50.
[34] Y.-S. Lee, J.-S. Ryou, Self healing behavior for crack closing of expansive agent via granulation/film coating method, Construct. Build. Mater. 71 (2014) 188–193.
[35] Y.-S. Lee, J.-S. Ryou, Crack healing performance of PVA-coated granules made of cement, CSA, and Na2CO3 in the cement matrix, Materials 9 (7) (2016) 555.
[36] J. Feng, H. Dong, R. Wang, Y. Su, A novel capsule by poly (ethylene glycol) granulation for self-healing concrete, Cement Concr. Res. 133 (2020).
[37] Y. Sumra, S. Payam, I. Zainah, The pH of cement-based materials: a review, J. Wuhan Univ. Technol.-Materials Sci. Ed. 35 (5) (2020) 908–924.
[38] RILEM, Test Method No. II 4, Water Absorption Tube Test, RILEM, 2006.
[39] Z. Jiang, W. Li, Z. Yuan, Influence of mineral additives and environmental conditions on the self-healing capabilities of cementitious materials, Cement Concr. Compos. 57 (2015) 116–127.
[40] E. Tziviloglou, V. Wiktor, H.M. Jonkers, E. Schlangen, Bacteria-based self-healing concrete to increase liquid tightness of cracks, Construct. Build. Mater. 122 (2016) 118–125.
[41] Q. Li, Z. Liu, W. Chen, B. Yuan, X. Liu, W. Chen, A novel bio-inspired bone-mimic self-healing cement paste based on hydroxyapatite formation, Cement Concr. Compos. 104 (2019).
[42] S. Kang, J. Peng, F. Zhou, X. Liu, Study on influence of hydroxy propyl methylcellulose ester and sand ratio on properities of full lightweight Aggregate concrete, Bullet. Chinese Ceram. Soc. 32 (10) (2013) 2003–2007.
[43] Y. Zhang, D. Sun, H. Qin, Civil Engineering Materials, Southeast University Press, 2013.
[44] G. Hong, S. Choi, Rapid self-sealing of cracks in cementitious materials incorporating superabsorbent polymers, Construct. Build. Mater. 143 (2017) 366–375.
[45] G. Hong, C. Song, J. Park, S. Choi, Hysteretic behavior of rapid self-sealing of cracks in cementitious materials incorporating superabsorbent polymers, Construct. Build. Mater. 195 (2019) 187–197.
[46] H.X.D. Lee, H.S. Wong, N.R. Buenfeld, Effect of alkalinity and calcium concentration of pore solution on the swelling and ionic exchange of superabsorbent polymers in cement paste, Cement Concr. Compos. 88 (2018) 150–164.
[47] M. Maciejewski, H.R. Oswald, A. Reller, Thermal transformations of vaterite and calcite, Thermochim. Acta 234 (1994) 315–328.